JOURNAL OF VIROLOGY, Jan. 1997, p. 562–568 Vol. 71, No. 1
0022-538X/97/$04.00+0


# Improvement of the Specific Infectivity of the Rubella Virus (RUB) Infectious Clone: Determinants of Cytopathogenicity Induced by RUB Map to the Nonstructural Proteins

KONSTANTIN V. PUGACHEV, EMILY S. ABERNATHY, AND TERYL K. FREY*

*Department of Biology, Georgia State University, Atlanta, Georgia 30303*

Received 19 June 1996/Accepted 27 September 1996

**A plasmid, Robo102, which contains a cDNA copy of the rubella virus (RUB) genomic RNA from which infectious transcripts can be synthesized in vitro, was recently developed (C. Y. Wang, G. Dominguez, and T. K. Frey, J. Virol. 68:3550–3557, 1994). To increase the specific infectivity of Robo102 transcripts (~5 plaques/10 μg of transcripts), a modified reverse transcription-PCR method was used to amplify nearly 90% of the RUB genome in three fragments, which were then used to replace the corresponding fragments in Robo102. Replacement of a fragment covering nucleotides (nt) 5352 to 9759 of the RUB genome yielded a construct, Robo202, which produced highly infectious transcripts ($10^4$ plaques/μg), indicating the presence of an unrecognized deleterious mutation (or mutations) in this region of the Robo102 cDNA. Robo102 was based on the w-Therien strain of RUB, which forms opaque plaques in Vero cells, while the PCR replacement fragments were generated from a variant, f-Therien, which produces clear plaques in Vero cells. Although Robo202 contains over 4,000 nt from f-Therien, Robo202 virus produces opaque plaques. However, when the other two PCR fragments amplified from f-Therien (nt 1 to 1723 and nt 2800 to 5352) were introduced into Robo202, the resulting construct, Robo302, yielded transcripts that produced a virus that formed clear plaques. This indicates that the determinants of plaque morphology map to the regions of the genome covered by these two fragments, both of which are in the nonstructural open reading frame. Generation of Robo202/302 chimeras indicated that the most 5′ terminal fragment (nt 1 to 1723) had the greatest effect on plaque morphology. The plaque morphology was correlated with the ability of the viruses to kill infected cells. The only difference at the molecular level detected among the viruses was that the more cytopathic viruses produced more nonstructural proteins than did the less cytopathic viruses. This finding, as well as the mapping of the genetic determinants to the region of the genome encoding these proteins, indicates that the nonstructural proteins can mediate cell killing.**

Rubella virus (RUB) is the sole member of the *Rubivirus* genus of the *Togaviridae* family of animal viruses, whose only known natural host is humans (reviewed in reference 7). The RUB virion consists of an icosahedral nucleocapsid surrounded by a lipid bilayer of cellular origin in which are embedded two virus-specified glycoproteins, E1 and E2. The nucleocapsid is composed of multiple copies of a virus-specified capsid protein, C, and contains single-stranded, positive-polarity genomic RNA of roughly 10,000 nucleotides (nt). In the cytoplasm of infected cells, the genomic RNA functions as an mRNA to produce a polyprotein precursor that is posttranslationally cleaved into the two virus nonstructural proteins, P150 and P90, that function in virus RNA replication. The open reading frame encoding the nonstructural proteins (NSP-ORF) occupies the 5′-terminal two-thirds of the genome. The genomic RNA also serves as a template for synthesis of a complementary minus-strand RNA, which, in turn, is the template for synthesis of genomic RNA as well as a subgenomic RNA. The subgenomic RNA functions as an mRNA for the RUB structural proteins (C, E2, and E1), which are encoded by an ORF (SP-ORF) contained within the 3′-terminal one-third of the genome. Synthesis of the subgenomic RNA is initiated on the minus-strand template at a site located between the two ORFs.

We determined the entire nucleotide sequence of the genome of a wild-type RUB strain, w-Therien (5), and constructed a so-called infectious clone (Robo102) from clones used in sequence determination (19). The Robo102 plasmid contains a complete cDNA copy of the w-Therien genome, which can be transcribed in vitro by using bacteriophage SP6 RNA polymerase to produce genomic transcripts. A problem encountered with Robo102 was the low infectivity of the transcripts (~5 plaques/10 μg of transcripts) (19). A likely reason for the low infectivity was the presence of unrecognized deleterious mutations in the Robo102 genomic cDNA. Similar problems have been encountered with infectious clones of other viruses (e.g., the Sindbis virus infectious clone [17]). To overcome this problem, the present study was initiated to amplify the RUB genome in a minimum number of fragments by using recently developed PCR techniques with which long sequences can be amplified (1, 3) and to use these fragments to replace the corresponding regions in Robo102.

A fundamental question in virology is how viruses kill cells. With RUB, as well as with the majority of other viruses, the molecular basis of cell killing is unknown. In most mammalian cell lines, RUB replicates noncytopathically; however, in a few cell lines (Vero, BHK-21, and RK-13) cytopathic effect (CPE) is induced and RUB can form plaques (reviewed in reference 7). Differences in plaque morphology and extent of replication between RUB strains have been reported (10, 14). For the RUB strains used in our laboratory, the w-Therien strain of RUB on which Robo102 was based induces moderate CPE and forms opaque plaques in Vero cells and transfection of Vero cells with Robo102 transcripts resulted in the formation of opaque plaques (19). As a template for long PCR, we used a

* Corresponding author.

variant of the w-Therien strain, called f-Therien, which was obtained by selection of a clear plaque from a plaque assay of w-Therien stock (18a). The f-Therien variant stably maintains its distinctive clear plaque phenotype and induces more profound CPE in infected Vero cells than does w-Therien. In the process of upgrading the specific infectivity of Robo transcripts, we generated several chimeras between the two Therien variants that expressed the difference in plaque morphology. These chimeras differed in the NSP-ORF region of the genome, indicating that this region determines the difference in plaque morphology.

## MATERIALS AND METHODS

**Cells and viruses.** Vero cells (obtained from the American Type Culture Collection) were maintained in Dulbecco's modified Eagle's medium (Gibco/BRL) containing 5% fetal bovine serum and gentamicin (10 μg/ml) at 35°C under 5% $CO_2$. The w-Therien strain of RUB, originally obtained from J. Wolinsky, and the f-Therien strain of RUB, originally obtained from J. Chantler, were propagated as described previously (6, 11, 19). Plaque assays and trypan blue exclusion tests were done as described previously (11, 19).

**Preparation of f-Therien virion RNA and RT-long PCR.** Monolayers of Vero cells grown in four 225-$cm^2$ flasks (roughly $4 \times 10^7$ cells/flask) were infected with f-Therien RUB at a multiplicity of infection (MOI) of 0.5 PFU/cell. At 4 days postinfection (when moderate CPE was observable), the culture medium was harvested and virion RNA was prepared by one of two methods. Briefly, in the first method (19), virions were precipitated from the medium with polyethylene glycol (PEG) and purified by centrifugation in a 25 to 50% discontinuous sucrose gradient. The virion band at the interphase was collected, digested with proteinase K, and phenol-chloroform extracted, and virion RNA was precipitated with ethanol. Alternatively, the PEG-precipitated virions were redissolved in 2.5 ml of phosphate-buffered saline and virion RNA was extracted with TRI-Reagent LS (Molecular Research Center, Cincinnati, Ohio) as specified by the manufacturer. Virion RNA recovered following each of the two extraction protocols was further purified by oligo(dT)-cellulose chromatography, redissolved in 50 μl of $H_2O$, and stored at −70°C.

First-strand cDNA synthesis was done with avian myeloblastosis virus reverse transcriptase from a RiboClone cDNA Synthesis System kit (Promega) as specified by the manufacturer (in the presence of sodium pyrophosphate). In each 20-μl reaction mixture, 5 μl of virion RNA was used as a template. First-strand syntheses were primed with 0.5 μg of one of three oligonucleotides: 5′-GGGA AGCTTGCACGACACGGACAAAAGCC (oligonucleotide 79; the underlined sequence is complementary to nt 1897 to 1916 of the RUB genome [numbering as in reference 5], and the resulting single-stranded product was subsequently used to generate PCR fragment I [see Fig. 1]), 5′-TAGTCTTCGGCGCAAGG (oligonucleotide 125; complementary to nt 5744 to 5760; PCR fragment II), and 5′-CGCGAATTC$(T)_{20}$CTATACAGCAACAGGTGC (oligonucleotide F1; contains an *Eco*RI site [doubly underlined], a $dT_{20}$ stretch, and a sequence complementary to nt 9740 to 9757 [singly underlined]; PCR fragment III). The single-stranded products were phenol-chloroform extracted and precipitated twice with ethanol, first in the presence of 2 M ammonium acetate and second in the presence of 0.3 M sodium acetate. The precipitates were redissolved in 10 μl of $H_2O$, and 2 to 5 μl was used in 50-μl PCRs that contained 2.5 U of ExTaq temperature-stable DNA polymerase (TaKaRa LA PCR kit; Pan Vera Corp., Madison, Wis.) in buffer provided by the manufacturer and supplemented with 10% dimethyl sulfoxide DMSO, 5.76 mM β-mercaptoethanol, and 0.1 mg of bovine serum albumin per ml. The following pairs of primers and amplification protocols were used: for fragment I (see Fig. 1), 5′-TCGAAGCTTATTTAGG TGACACTATAGCAATGGAAGCTATCGGACCTCGCTTAGG (oligonucleotide F2; contains a *Hin*dIII site [doubly underlined], the SP6 RNA polymerase promoter [dot underline], and nt 1 to 28 of the RUB genome [singly underlined]) and oligonucleotide 79, 30 cycles of 20 s at 98°C, 1 s at 55°C, and 3 min at 70°C; for fragment II, 5′-TTTGCCAACGCCACGGC (oligonucleotide 251, containing nt 2600 to 2616) and oligonucleotide 125, 30 cycles of 20 s at 98°C, 1 s at 50°C, and 5 min at 70°C; and for fragment III, 5′-AGCTCACCGACCGCTAC (oligonucleotide 106, containing nt 5319 to 5335) and oligonucleotide F1, 30 cycles of 20 s at 98°C, 1 s at 52°C, and 7 min at 68°C. The resulting PCR fragments were purified with QIAquick Spin PCR purification kit (QIAGEN Inc., Chatsworth, Calif.) and recovered in 50 μl of water.

**Analysis to determine which fragment conferred improvement of infectivity and construction of plasmids.** In these protocols, standard recombinant DNA techniques were used (13) with minor modifications. Enzymes were obtained from New England BioLabs or Boehringer Mannheim Biochemicals.

To determine which of the three PCR fragments would improve the infectivity of the Robo102 transcripts, fragments I, II, and III were digested with *Hin*dIII and *Kpn*I, *Nhe*I and *Bgl*II, or *Bgl*II and *Eco*RI, respectively, and ligated with Robo102 from which the corresponding fragment had been removed (see Fig. 1). Each ligation reaction mixture contained 1 μg of DNA composed of roughly equimolar amounts of the fragments. Following overnight incubation at 14°C, the DNAs were digested with *Eco*RI, phenol-chloroform extracted, and used for in vitro transcription followed by Lipofectin-mediated transfection of Vero cells. The transfected cells were incubated and observed for the appearance of RUB-induced CPE.

Subsequently, Robo202 was generated by introduction of fragment III into Robo102. Then fragments I and II were introduced in one step into Robo202, producing Robo302. Robo202/I and Robo202/II plasmids were obtained by exchanging the corresponding regions between Robo202 and Robo302. In these manipulations, WM1100 (a $RecA^-$ derivative of MC1061 [obtained from S. Schlesinger]) was used as the host strain. Robo102 is based on the low-copy-number, spectinomycin-resistant vector pCL1921 (12, 19), and thus selection for and growth of plasmid-containing cells were done in the presence of 50 μg of spectinomycin per ml. Plasmids were extracted from bacteria by the alkaline procedure and purified by CsCl-gradient ultracentrifugation. Sequencing was done with a dideoxy chain termination sequencing kit (United States Biochemicals, Cleveland, Ohio).

**In vitro transcription and transfection of Vero cells.** Linearization for runoff transcription was done with *Eco*RI. A 1-μg sample of in vitro ligation products or linearized plasmid was transcribed in vitro with SP6 RNA polymerase (Epicentre Technologies) in the presence of $m^7G(5')ppp(5')G$ cap structure analog (New England BioLabs) as described previously (16). For such reactions, we use freshly linearized Robo plasmids, since linearized plasmids stored at −20°C exhibited decreased yields of transcripts. In indicated experiments, no cap analog, G(5′)ppp(5′)G, or G(5′)ppp(5′)A (New England BioLabs) was used instead of $m^7G(5')ppp(5')G$. The transcripts were analyzed by electrophoresis of aliquots of the reaction mixtures in 1% agarose gels in the presence of ethidium bromide. In some experiments, precise yields of the transcripts were determined spectrophotometrically. Typical yields were 6 to 7 μg of RNA per 25-μl reaction mixture containing 1 μg of linearized Robo plasmid. Lipofectin-mediated transfections of Vero cells grown in 60-mm plates were done by the method of Rice et al. (18) with the modification that Opti-MEM I reduced-serum medium was used instead of phosphate-buffered saline. To determine the efficiency of transfection, 10-fold serial dilutions of transcripts with known concentrations of RNA were made in Opti-MEM I prior to the addition of Lipofectin. The transfected monolayers were then overlaid with agar, and plaques were visualized on days 5 to 6 posttransfection. To produce virus stocks for replication studies, transfected cells were incubated in growth medium. Following development of significant CPE, the medium was harvested and virus was amplified by one passage in Vero cells.

**Sequencing of 5′ termini of virion RNA.** RUB virions were PEG precipitated from 5 ml of infected culture medium and redissolved in 250 μl of TNE buffer (10 mM Tris-HCl [pH 7.5], 100 mM NaCl, 1 mM EDTA). Virion RNA was isolated with TRI-Reagent LS (Molecular Research Center) as specified by the manufacturer (10 μg of glycogen was added prior to RNA precipitation) and redissolved in 10 μl of water. First-strand cDNA synthesis was done at 45°C for 1 h in a 20-μl reaction mixture containing 5 μl of virion RNA, 0.1 μg of oligonucleotide 36 (5′-TGGTCTCTTACCCAACT) complementary to nt 101 to 117 of the RUB genome, and 200 U of SuperScript II RNase $H^-$ Reverse Transcriptase (Gibco/BRL) in buffer provided by the manufacturer, containing 1 mM deoxynucleoside triphosphates and 1 U of RNasin (Promega) per μl. Then 1 μg of RNase I was added, and the reaction mixture was boiled for 1 min and incubated at room temperature for 5 min. The primer extension product was purified with a QIAquick Spin PCR purification kit (QIAGEN Inc.) and 3′-terminally tailed with dATP by using terminal deoxynucleotidyltransferase (United States Biochemical). The poly(A)-tailed primer extension product was phenol-chloroform extracted and precipitated twice with ethanol, first in the presence of 2 M ammonium acetate and second in the presence of 0.3 M sodium acetate. The precipitate was redissolved in 10 μl of $H_2O$, and 5 μl was used in a 50-μl PCR that contained 0.5 μg each of oligonucleotide 51 [5′-ACGTGCATG CCTGCAG$T_{20}$, which contains an oligo(dT) tail and a *Pst*I site (underlined)] and oligonucleotide 292 (5′-GTGTGAATTCTGGTCTCTTACCCAAC, which contains the same region complementary to the RUB genome as oligonucleotide 36 and an *Eco*RI site [underlined]) and 1 U of Deep Vent DNA polymerase (New England BioLabs) in buffer provided by the manufacturer and supplemented with 200 μM deoxynucleoside triphosphates. The amplification protocol consisted of one cycle of 1 min at 92°C, 1 min at 45°C, and 1 min at 72°C followed by three cycles of 1 min at 45°C and 1 min at 72°C (Deep Vent DNA polymerase was added at the 45°C step of the last of these cycles) and 29 cycles of 1 min at 92°C, 1 min at 55°C, and 1 min at 72°C. The PCR amplification product of roughly 150 nt was digested with *Eco*RI and *Pst*I and cloned into the pGEM1 vector. Several isolates of the resulting plasmid were sequenced.

**Northern blot hybridization and radioimmunoprecipitation.** Vero cells grown in 24-well plates were infected at an MOI of 2 PFU/cell. At 22 and 40 h postinfection, total intracellular RNA was extracted from each well with TRI-Reagent as specified by the manufacturer (Molecular Research Center). Aliquots of the extracted RNAs were analyzed by Northern blot hybridization as described previously (4). [$^{32}$P]dCTP nick-translated Robo102 plasmid was used as a probe for total RUB-specific RNAs, and [$^{32}$P]UTP-labeled Robo302 RNA transcripts were used as a probe for minus-strand RNA.

For analysis of virus protein production, Vero cells grown in 60-mm plates (Corning) were infected at an MOI of 2 PFU/cell. At the indicated times postinfection, the cells were radiolabeled for 1.5 h with [$^{35}$S]methionine (Amersham;

1,000 Ci/mmol) and lysed in 1 ml of RIPA buffer (16). Aliquots (200 μl) of these lysates were mixed with 2 μl of a mixture of monoclonal antibodies E1-20, E2-1, C2, and C8 (20) to immunoprecipitate the RUB structural proteins. Aliquots (800 μl) of the lysates were mixed with 5 μl of a mixture of rabbit polyclonal antisera GU1 and GU8 (6) to immunoprecipitate the nonstructural proteins of RUB (antipain dihydrochloride protease inhibitor [Boehringer Mannheim] was also added to 74 μM). The immune complexes were recovered with protein A-Sepharose beads (Pharmacia), boiled for 2 min in sodium dodecyl sulfate (SDS) sample loading buffer, and resolved by SDS-polyacrylamide gel electrophoresis (7.5 to 25% polyacrylamide gradient), and the dried gels were autoradiographed. To measure quantities of radioactivity present in the protein (or RNA) bands, the gels (or the hybridized filters) were analyzed in a Fujix BAS1000 bioimaging analyzer (Fuji Photo Film, Tokyo, Japan) with software provided by the manufacturer.

## RESULTS

**Restriction fragment replacement in Robo102 by RT-long PCR.** To overcome the problem of low infectivity of Robo102 transcripts, we used a modified RT-long PCR technique (1, 3) to amplify roughly 90% of the f-Therien RUB genome in three fragments. An unusual feature of the RUB genome is its G+C content of nearly 70% (5, 7), which makes lengthy RUB sequences difficult to amplify by PCR. To overcome this difficulty, we routinely add 10% DMSO to PCR amplifications of RUB sequences. We find that *Taq* DNA polymerase retains full activity in 10% DMSO whereas Deep Vent DNA polymerase (New England BioLabs) does not. However, in our experience, addition of 10% DMSO also leads to a very high rate of mutations introduced by *Taq* polymerase (1 mutation per 100 to 300 nucleotides amplified). The RT-long PCR procedure utilizes thermostable ExTaq DNA polymerase that has a 3′ → 5′ exonuclease proofreading activity. We found that ExTaq polymerase also requires 10% DMSO to amplify large fragments of the RUB genome and is fully active in the presence of 10% DMSO. To assess the proofreading activity of the enzyme in the presence of 10% DMSO, a 938-bp fragment (*Pst*I-*Bam*HI, nt 8227 to 9165) of the RUB sequence amplified from the Robo102 template with ExTaq polymerase was cloned into pGEM1 plasmid vector and sequences of three independent clones were determined (a total in excess of 2,700 nt), with the result that no changes were detected. Thus, the enzyme retains proofreading activity in 10% DMSO.

We found three pairs of primers which could be used to efficiently amplify three specific fragments of 1920 to 4430 nt that spanned convenient restriction sites for insertion into Robo102 (Fig. 1). We found that for successful amplification, template virion RNA had to be purified by oligo(dT) cellulose chromatography. Interestingly, we were unable to amplify a PCR fragment that covered the region between *Kpn*I (nt 1723) and *Nhe*I (nt 2800) sites (Fig. 1), either from virion RNA or from Robo102 template, presumably due to peculiarities of secondary and/or tertiary structure in this region.

The three PCR fragments were then tested individually for their ability to improve the infectivity of Robo102 transcripts. Each fragment digested with appropriate restriction enzymes was ligated into Robo102, and aliquots of the ligation mixtures were linearized by digestion with *Eco*RI and directly transcribed in vitro. The transcripts were used to transfect Vero cells. The ligation that contained PCR fragment III led to CPE within 5 days; the other ligations, as well as the Robo102 control, did not induce CPE within 8 days (the specific infectivity of Robo102 transcripts of ~5 plaques/10 μg was measured in BHK cells [19]; the efficiency of transfection is lower in Vero cells, and thus transfection with Robo102 transcripts frequently led to recovery of no virus). This indicated that the deleterious mutation(s) in Robo102 is between nt 5352 (*Bgl*II site) and the 3′ end of the genome. Therefore, the remainder of the Robo102-PCR fragment III ligation mixture was used to

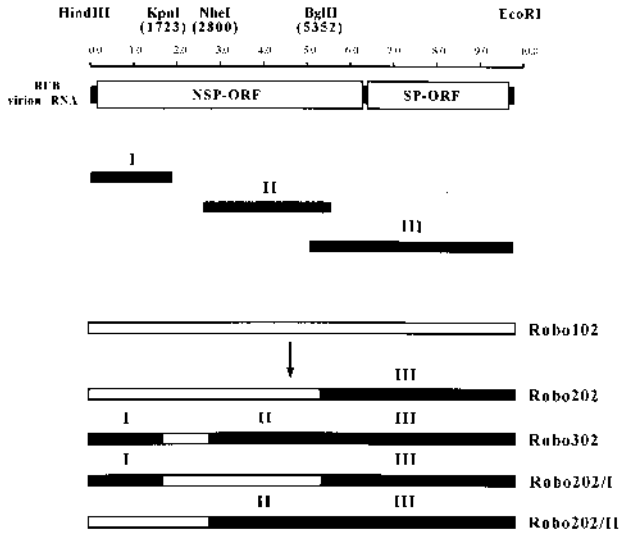


FIG. 1. Construction of Robo202/302 plasmids. Roughly 90% of the RUB genome (top diagram) was amplified in three fragments (I, II, and III) by a modified RT-long PCR technique with purified f-Therien RUB virion RNA as a template. The three PCR products were then used to replace the corresponding regions in Robo102 plasmid, which was based on w-Therien RUB (19), to produce the constructs shown. First, PCR fragment III was introduced into Robo102 to generate Robo202. PCR fragments I and II were then introduced in one ligation step into Robo202, resulting in Robo302. Robo202/I and Robo202/II were obtained by introduction of fragments I and II, respectively, derived from Robo302 into Robo202.

transform *E. coli* cells. Plasmids from 32 colonies were transcribed in vitro, and the transcripts were used to transfect Vero cells; transcripts from two of these plasmids yielded virus. One of these, designated Robo202, was used for further manipulations. PCR fragments I and II were introduced into Robo202 in one ligation step. Of 23 resulting plasmids tested, 1 yielded infectious transcripts that induced CPE that appeared more rapidly and was more pronounced than the CPE induced by Robo202 (2 plasmids produced less pronounced CPE than Robo202, and 20 did not produce CPE). This plasmid was designated Robo302. Subsequently, fragments I and II derived from Robo302 were introduced individually into Robo202 to produce Robo202/I and Robo202/II, respectively. With regard to the low proportion of "successful" plasmids in these experiments (2 plasmids of 32 clones analyzed and 1 plasmid of 23 clones for Robo202 and Robo302, respectively), since ExTaq polymerase retains its high fidelity in the long PCR amplification protocol used, it is possible that this is due to heterogeneity of the virion RNA template population or mistakes by avian myeloblastosis virus reverse transcriptase during first-strand cDNA synthesis on the high-G+C-content RNA template.

The specific infectivity of both Robo202 and Robo302 transcripts in Vero cells is roughly $10^4$ plaques/μg. In comparison, we find that the specific infectivity in Vero cells of transcripts of Toto1101, a Sindbis virus infectious clone (17), is $5 \times 10^4$ plaques/μg. To determine whether the infectivity was stable during propagation of the Robo plasmids in *E. coli* WM1100 cells, an initial minipreparation of Robo202 and a large-scale preparation of Robo302 were used for transformation of bacteria. Plasmids isolated from a total of 13 different colonies were individually transcribed in vitro, and Vero cells were transfected with the resulting RNA transcripts. All 13 transfections resulted in CPE within 4 to 5 days posttransfection. We have also made four independent large-scale preparations

TABLE 1. Specific infectivity of Robo302 transcripts: effect of cap structure[a]

| RNA used for transfection | Specific infectivity (plaques/μg) |
|---|---|
| Robo302 transcripts | |
| No cap[b] | 0 |
| $m^7G(5')ppp(5')G$[c] | $10^4$ |
| $A(5')ppp(5')G$[d] | $3 \times 10^3$ |
| $G(5')ppp(5')G$[d] | $0.6 \times 10^3$ |
| RUB virion RNA[e] | $9.3 \times 10^4$ |

[a] The specific infectivity was determined by using serial 10-fold dilutions of the in vitro RNA transcripts. Monolayers of Vero cells were transfected with Lipofectin and overlaid with plaque assay agar. Plaques were visualized on day 6 posttransfection.
[b] The transcripts were synthesized in the absence of cap analog. In three independent experiments, no plaques were observed.
[c] The mean value of three independent experiments is given.
[d] The result of one experiment is given.
[e] The infectivity of purified RUB virion RNA was determined previously (19).

of Robo302 (each starting from a different colony), all of which yield infectious transcripts.

**Effect of cap structure, the additional 5′ G, and poly(A)-tail length on infectivity of Robo transcripts.** As shown in Table 1, the specific infectivity of Robo302 RNA transcripts synthesized in the presence of $m^7G(5')ppp(5')G$ cap analog is $10^4$ plaques/μg. We also tried two other commercially available cap analogs, $G(5')ppp(5')G$ and $A(5')ppp(5')G$. In vitro transcripts synthesized in the presence of these caps were also infectious but had a lower specific infectivity. In three independent experiments, no plaques were detected when the cells were transfected with Robo302 transcripts synthesized in the absence of cap analog, indicating that the cap structure at the 5′ end of the transcripts is an absolute requirement for transcript infectivity. This is consistent with the findings of Oker-Blom et al. (15), who reported the presence of a caplike structure on virion RNA of RUB (the specific type of cap and the nucleotides within the structure were not identified).

The Robo transcripts start with an additional G residue at their 5′ ends that is contributed by the last nucleotide of the SP6 promoter; the first nucleotide of the RUB genome is C (19). To learn the fate of this extra G, we determined the 5′ termini of virion RNA from preparations of Robo302 virus harvested following one and five passages of the virus obtained after transfection. After one passage, 60% of 5′-terminal clones still had the extra G, but after five passages, no clones containing the extra G were found. After five passages, plaques of the virus appeared to be larger and the virus grew to a higher titer than did the virus harvested after one passage (data not shown); to what extent this was correlated with the loss of the extra G is not known.

The Robo202/302 constructs all contain a 20-nt poly(A) tract at the 3′ end of the RUB cDNA preceding the *Eco*RI linearization site. The mean length of the poly(A) tail in the RUB genomic RNA is 53 nt, and Robo102 has a 52-nt poly(A) tract (19). We produced a Robo202 derivative in which the length of the poly(A) tract was increased from 20 to 40 nt; however, this did not lead to an increase in specific infectivity.

**Phenotypic differences between Robo202 and Robo302: association with the nonstructural region of the genome.** As discussed above, Robo102 was derived from the w-Therien strain, which forms opaque plaques, while the f-Therien variant, which forms clear plaques, was used in construction of Robo202 and Robo302. Although both Robo202 and Robo302 contain the same 3′-terminal 4405 nt derived from f-Therien, Robo202 virus forms opaque plaques, as does w-Therien virus, while Robo302 virus forms clear plaques similar to f-Therien plaques although somewhat smaller (Fig. 2). The difference in plaque morphology between Robo202 and Robo302 is thus associated with the nonstructural (5′-terminal) part of the RUB genome, the region of the genome in which these two constructs differ.

Two PCR fragments (I and II [Fig. 1]) from the nonstructural region of the f-Therien genome were used in construction of Robo302 from Robo202. As can be seen in Fig. 2, Robo202/I virus, which contains only fragment I, forms clear plaques that are slightly smaller than Robo302 plaques, while Robo202/II virus, which contains only fragment II, forms plaques that are the same size as Robo202 and Robo302 plaques and somewhat less opaque than Robo202 plaques. Thus, both fragments appear to contain determinants that affect plaque morphology; however the contribution by fragment I is more pronounced. The nucleotide sequences of the fragment I and II regions from both Robo302 and Robo202 plasmids were determined. A summary of the differences is given in Table 2. Fragments I and II of Robo202 and Robo302 differ at 10 and 7 nucleotide residues, respectively. Seven of these differences in fragment I and five in fragment II lead to amino acid substitutions in the NSP-ORF.

To elucidate the basis of the difference in plaque phenotype between the Robo constructs, we determined the growth curves of these viruses and their ability to kill infected cells. Because of the limited titer to which one of the viruses (Robo202/I) replicates, an MOI of 2 PFU/cell was used in these experiments. The growth curves are shown in Fig. 3. As can be seen, the growth kinetics of all of these viruses were similar, with a lag phase of roughly 12 h, an exponential phase between 12 and 24 h postinfection, and a slower exponential phase through 55 h postinfection. f-Therien produced the highest titers, while w-Therien, Robo302, Robo202, and Robo202/

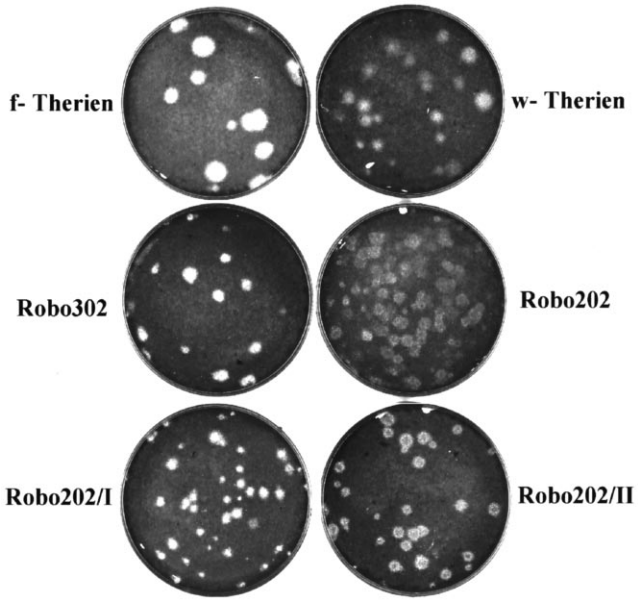


FIG. 2. Plaque morphology of f- and w-Therien RUB and the Robo202/302 chimeras. Monolayers of Vero cells grown in 60-mm plates were infected with indicated viruses, overlaid with 5 ml of agar (0.4% agar [Oxoid no. 1] in Eagle's minimal essential medium, 1% fetal bovine serum, 0.1% DEAE-dextran, and 10 μg of gentamicin per ml), and incubated at 35°C under 5% $CO_2$. Plaques were visualized by staining with 0.1% crystal violet in 4% formalin on day 6 postinfection.

TABLE 2. Summary of nucleotide differences in fragments I and II between Robo202 and Robo302[a]

| Nucleotide position | Fragment | Nucleotide in: | | Codon change[b] | |
|---|---|---|---|---|---|
| | | Robo202 | Robo302 | Residue no. | Change |
| 49 | I | A | G | 3 | — |
| 431 | I | A | G | 131 | S→G |
| 775 | I | C | T | 245 | — |
| 1124 | I | T | A | 362 | C→S |
| 1334 | I | C | T | 432 | L→F |
| 1509 | I | A | C | 490 | E→A |
| 1578 | I | A | C | 513 | Q→P |
| 1691 | I | C | T | 551 | P→S |
| 1701 | I | C | T | 554 | P→L |
| 1708 | I | A | C | 556 | — |
| 3162 | II | A | G | 1041 | Y→C |
| 3382 | II | T | G | 1114 | H→Q |
| 3713 | II | G | A | 1225 | A→T |
| 3778 | II | T | C | 1246 | — |
| 4217 | II | A | T | 1393 | I→F |
| 4436 | II | C | A | 1466 | R→S |
| 4441 | II | G | A | 1467 | — |

[a] Fragments I and II of Robo302 and Robo202 (Fig. 1) were sequenced, and the resulting sequences were compared. Nucleotide and amino acid residue numbering is that of Dominguez et al. (5).

[b] Amino acid differences in the NSP-ORF (Robo202→Robo302) resulting from nucleotide differences. —, means no change (silent mutation).

TABLE 3. Average titers produced by Therien and Robo viruses[a]

| Virus | Titer (PFU/ml) |
|---|---|
| f-Therien | $2.6 \times 10^7$ |
| w-Therien | $2.5 \times 10^7$ |
| Robo302 | $1.4 \times 10^7$ |
| Robo202 | $1 \times 10^7$ |
| Robo202/I | $1.36 \times 10^6$ |
| Robo202/II | $1.2 \times 10^7$ |

[a] Vero cells were infected at an MOI of 2 PFU/cell. Media were collected on day 4 postinfection, and the titers of the virus preparations were determined. Mean values of titers produced in two independent experiments are given.

II produced similar, intermediate titers. Robo202/I virus grew to noticeably lower titers than the other viruses. Over a more prolonged course of infection (4 days), w-Therien titers caught up with f-Therien titers; Robo202, Robo302, and Robo202/II titers were approximately 2-fold lower than f- and w-Therien titers; and Robo202/I titers were 8- to 18-fold lower than those of any of the other viruses (Table 3). Thus, clear plaque morphology is not correlated with the level of virus production.

When cell viability in cultures infected by these viruses was assayed by trypan blue exclusion, f-Therien was found to induce a higher level of cell death (~10% viability compared to the mock-infected control) than w-Therien (~40%) (Fig. 4). This level of cell viability in Vero cells infected with w-Therien is similar to observations in an earlier study (11). Correspondingly, Robo302 virus was a more efficient inducer of cell death (~20% cell survival) than was Robo202 (~60%). Therefore, the plaque phenotype difference is correlated with the ability of these viruses to kill infected cells.

To analyze molecular differences between these viruses that could account for the difference in plaque morphology and cell killing, virus macromolecular synthesis was characterized. Production of the RUB-specific RNAs (of both positive and negative polarities) was examined by Northern blot hybridization of total intracellular RNAs extracted from infected cells, with the result that all of these viruses produced equivalent amounts of all the virus RNA species (data not shown). NSP and SP synthesis was analyzed by immunoprecipitation of the proteins from lysates of infected cells radiolabeled for 1.5 h. As shown in Fig. 5A, SP synthesis was similar for all of the viruses. However, production of the NSPs (Fig. 5B and C) was higher in cells infected with the more cytopathic viruses (f-Therien and Robo302) than in those infected with the less cytopathic viruses (w-Therien and Robo202). Robo202/I also produced more NSP than did Robo202/II. These differences were not due to differences in the number of infected cells in the culture, since at 40 h postinfection a similar percentage of cells (roughly 60%) was infected with f-Therien, w-Therien, Robo302, Robo202, and Robo202/II viruses as determined by indirect immunofluorescence (results not shown). However, only 35% of Robo202/I-infected cells were infected, probably due to the slower replication of this virus. Therefore, the amount of NSPs

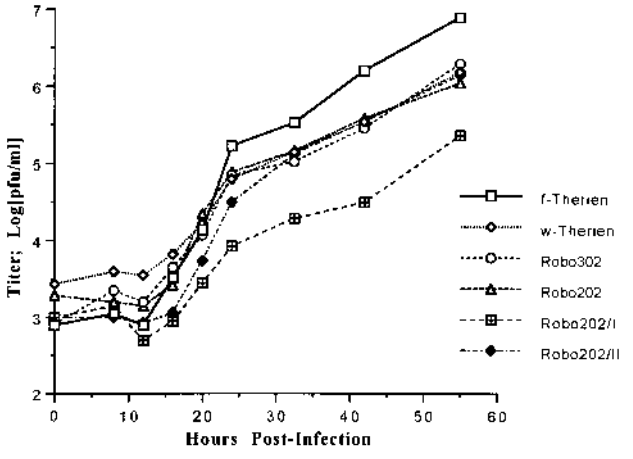


FIG. 3. Growth curves of f- and w-Therien RUB and the Robo202/302 viruses. Vero cells were infected with the indicated viruses at an MOI of 2 PFU/cell. At various times postinfection, 50-μl aliquots of the infected culture media were harvested and stored at −70°C prior to titer determination on Vero cells. The graph shows mean values of titers determined in two independent experiments.

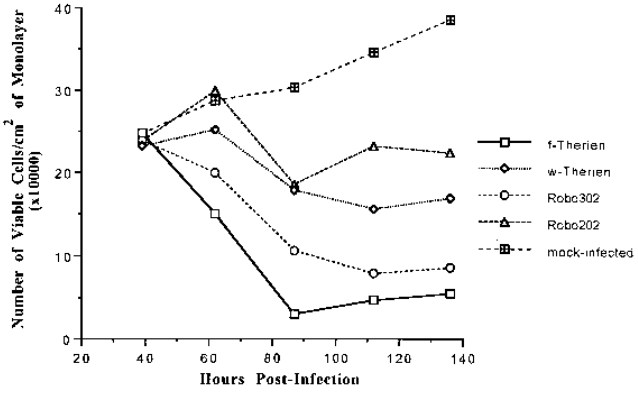


FIG. 4. Viability of Vero cells infected by f-Therien, w-Therien, Robo302, and Robo202 viruses. Vero cells grown in 24-well plates were infected with the indicated viruses at an MOI of 2 PFU/cell. At the indicated times postinfection, cells were trypsinized, washed with phosphate-buffered saline, and mixed with 0.4% trypan blue stain (Gibco/BRL) before live cells were counted. To ensure statistical accuracy, three aliquots of each trypsinized cell suspension were counted.

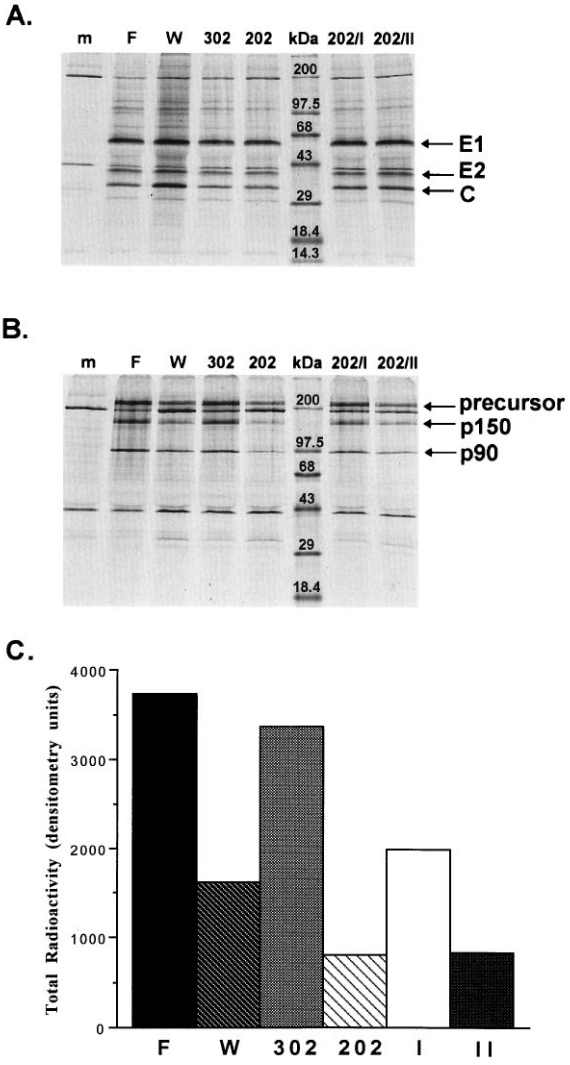


FIG. 5. (A and B) Production of the RUB SPs (A) and NSPs (B). Vero cells were mock infected (lanes m) or infected with f-Therien, w-Therien, Robo302, Robo202, Robo202/I, or Robo202/II (lanes F, W, 302, 202, 202/I, and 202/II, respectively) at an MOI of 2 PFU/cell. At 40 h postinfection, the cells were radiolabeled for 1.5 h with [$^{35}$S]methionine and lysed in RIPA buffer. The RUB proteins were immunoprecipitated and resolved by SDS-polyacrylamide gel electrophoresis (7.5 to 25% polyacrylamide gradient). Positions of each of the RUB-specific proteins are indicated. Lanes kDa contain molecular mass standards. A similar result was obtained when the experiment was done at 22 h postinfection (results not shown). (C) Diagram of the total radioactivity present in all three NSP bands in the autoradiogram in panel B (precursor, p150, and p90) for each of the viruses. To determine these radioactivities, the gel was analyzed in a Fujix BAS1000 phosphoimager with the manufacturer's software.

produced by Robo202/I is probably underrepresent in the diagram in Fig. 5C.

## DISCUSSION

To date, full-length genomic cDNA clones that can be used for synthesis of infectious RNA transcripts in vitro or in vivo have been developed for over 40 different plant and animal plus-strand RNA viruses (reviewed in reference 2). Successful generation of infectious cDNA clones is a difficult and multistep process, which is often problematic due to the presence of mutations in the virus RNA template population as a result of the inherent mutability of RNA viruses, the relatively low fidelity of the DNA polymerases used in cDNA synthesis, the instability and toxicity of viral sequences in bacterial hosts, and the infidelity of the RNA polymerases used for in vitro transcriptions. A common result is the introduction of unrecognized lethal or deleterious mutations in the cDNA clone. These mutations are usually located and removed by restriction fragment replacement from a cDNA library. We used the recent technological development of high-fidelity long PCR to greatly facilitate this replacement process. By ligating the amplified products into the cDNA clone and directly transcribing without intermediate transformation, we were rapidly able to ascertain that infectivity was recoverable and localize the mutation. Since the mutation was in a large fragment derived from an alternate strain, we have not attempted to identify it. Subsequently, a stable infectious clone was recovered. The specific infectivity of transcripts ($10^4$ plaques/$\mu$g) was $10^4$-fold enhanced over the previous construct and approached the infectivity of the Sindbis virus infectious clone. This improved infectivity will greatly enhance the utility of the Robo constructs in the analysis of RUB replication.

The original infectious clone, Robo102, was constructed by using the w-Therien strain of RUB, which forms opaque plaques on Vero cells. In upgrading the specific infectivity of Robo102, we used a variant, f-Therien, that produces clear plaques, in hopes of obtaining a construct that would also produce clear plaques. Fortuitously, we were able to generate two constructs, Robo202 and Robo302, which expressed plaque phenotypes similar to the parental viruses (opaque and clear, respectively). We found that Robo302 and f-Therien killed a greater proportion of the infected cells than did Robo202 and w-Therien, explaining the difference in the plaque phenotypes. Since Robo202 and Robo302 contain the same 3′-terminal half derived from the f-Therien genome (fragment III) but differ in the two fragments (I and II) from the 5′-terminal part of the genome, the difference in plaque morphology of Robo202 and Robo302 is associated with the NSP-ORF. Presumably, this difference is due to genetic determinants in the parental w-Therien and f-Therien viruses. Of the Robo chimeras that contained either fragment I or fragment II, Robo202/I produced distinctly clearer plaques than did Robo202/II. Thus, a major determinant of plaque morphology appears to reside in fragment I sequences. However, important differences between Robo202 and Robo302 are present in fragment II as well as fragment I. First, Robo202/II also differed from Robo202 in plaque morphology. Furthermore, Robo202/I replicated less well than the other viruses, and thus some mutation that is necessary for Robo302 to replicate efficiently as well as to form clear plaques must exist in fragment II.

At the molecular level, we found that NSP synthesis was higher in cells infected with the more cytopathic viruses (Robo302 and f-Therien) than with the less cytopathic viruses (Robo202 and w-Therien) while production of the RUB-specific RNAs and SPs was similar. This correlates with mapping of the genetic determinants to the nonstructural region of the genome and suggests that the NSPs are involved in RUB-induced killing of Vero cells. Although these findings suggest that the level of NSP production is correlated with cytopathogenicity, we cannot exclude the possibility that some of the point mutations in the f-Therien NSPs cause more efficient cell killing. The simplest explanation for the different amounts of NSPs would be a difference in the efficiency of translation of the NSP-ORFs. In this regard, each virus that contained fragment I from f-Therien (Robo302 and Robo202/I) produced more of the NSPs than did the viruses with fragment I from w-Therien (Robo202 and Robo202/II). The 40-nt 5′ untrans-

lated region preceding the AUG initiation codon for the NSP-ORF is identical in f- and w-Therien and the Robo viruses, indicating that the difference in expression of the NSPs is associated with sequences located downstream from the initiation codon. A similar enhancing effect of sequences located downstream from the AUG initiation codon on the efficiency of translation was recently described for the subgenomic RNA of Sindbis virus (8, 9). With the availability of the pair of efficient infectious clones Robo202 and Robo302, it will be possible to determine the effect of individual nucleotides on both translation efficiency of the NSP-ORF and RUB-induced cell killing.

## ACKNOWLEDGMENTS

This study was supported by PHS grant AI-21389 from NIAID.

We thank Amy Zhao and Tim Brown for synthesis of oligonucleotides, Karen Lund for helpful technical suggestions, and Nancy Davis for critically reading the manuscript.

## REFERENCES

1. **Barnes, W. M.** 1994. PCR amplification of up to 35-kb DNA with high fidelity and high yield from λ bacteriophage template. Proc. Natl. Acad. Sci. USA **91:**2216–2220.
2. **Boyer, J.-C., and A.-L. Haenni.** 1994. Infectious transcripts and cDNA clones of RNA viruses. Virology **198:**415–426.
3. **Cheng, S., C. Fockler, W. M. Barnes, and R. Higuchi.** 1994. Effective amplification of long targets from cloned inserts and human genomic DNA. Proc. Natl. Acad. Sci. USA **91:**5695–5699.
4. **Derdeyn, C. A., and T. K. Frey.** 1995. Characterization of defective-interfering RNAs of rubella virus generated during serial undiluted passage. Virology **206:**216–226.
5. **Dominguez, G., C. Y. Wang, and T. K. Frey.** 1990. Sequence of the genome RNA of rubella virus: evidence for genetic rearrangement during Togavirus evolution. Virology **177:**225–238.
6. **Forng, R.-Y., and T. K. Frey.** 1995. Identification of the rubella virus nonstructural proteins. Virology **206:**843–853.
7. **Frey, T. K.** 1994. Molecular biology of rubella virus. Adv. Virus Res. **44:**69–160.
8. **Frolov, I., and S. Schlesinger.** 1994. Translation of Sindbis virus RNA: effects of sequences downstream of the initiating codon. J. Virol. **68:**8111–8117.
9. **Frolov, I., and S. Schlesinger.** 1996. Translation of Sindbis virus mRNA: analysis of sequences downstream of the initiating AUG codon that enhance translation. J. Virol. **70:**1182–1190.
10. **Gould, J. J., G. D. Laurence, and M. Butler.** 1972. An unusual plaque variant of rubella virus. J. Hyg. Camb. **70:**49–53.
11. **Hemphill, M. L., R.-Y. Forng, E. S. Abernathy, and T. K. Frey.** 1988. Time course of virus-specific macromolecular synthesis during rubella virus infection in Vero cells. Virology **162:**65–75.
12. **Lerner, C. G., and M. Inouye.** 1990. Low copy number plasmids for regulated low-level expression of cloned genes in *Escherichia coli* with blue/white insert screening capability. Nucleic Acids Res. **18:**4361.
13. **Maniatis, T., E. F. Fritsch, and J. Sambrook.** 1982. Molecular cloning: a laboratory manual, 2nd ed. Cold Spring Harbor Laboratory, Cold Spring Harbor, N.Y.
14. **Miki, N. P. H., and J. K. Chantler.** 1992. Differential ability of wild-type and vaccine strains of rubella virus to replicate and persist in human joint tissue. Clin. Exp. Rheumatol. **10:**3–12.
15. **Oker-Blom, C., I. Ulmanen, L. Kaarianen, and R. F. Petterson.** 1984. Rubella virus 40S genome RNA specifies a 24S subgenomic mRNA that codes for a precursor to structural proteins. J. Virol. **49:**403–408.
16. **Pugachev, K. V., P. W. Mason, and T. K. Frey.** 1995. Sindbis vectors suppress secretion of subviral particles of Japanese encephalitis virus from mammalian cells infected with SIN-JEV recombinants. Virology **209:**155–166.
17. **Rice, C. M., R. Levis, J. H. Strauss, and H. V. Huang.** 1987. Production of infectious RNA transcripts from Sindbis virus cDNA clones: mapping of lethal mutations, rescue of a temperature-sensitive marker, and in vitro mutagenesis to generate defined mutations. J. Virol. **61:**3809–3819.
18. **Rice, C. M., A. Grakoui, R. Galler, and T. J. Chambers.** 1989. Transcription of infectious yellow fever RNA from full-length cDNA templates produced by *in vitro* ligation. New Biol. **1:**285–296.

18a. **Salmi, A.** Personal communication.

19. **Wang, C. Y., G. Dominguez, and T. K. Frey.** 1994. Construction of rubella virus genome-length cDNA clones and synthesis of infectious RNA transcripts. J. Virol. **68:**3550–3557.
20. **Wolinsky, J. S., M. McCarthy, O. Allen-Cannady, W. T. Moore, R. Jin, S.-N. Cao, A. Lovett, and D. Simmons.** 1991. Monoclonal antibody-defined epitope map of expressed rubella virus protein domains. J. Virol. **65:**3986–3994.